



Rapid gravity filtration operational performance assessment and diagnosis for preventative maintenance from on-line data

A. Upton^a, B. Jefferson^a, G. Moore^b, P. Jarvis^{a,*}

^aCranfield Water Science Institute, Cranfield University, Cranfield, Bedfordshire MK43 0AL, UK

^bScottish Water, Castle House, 6 Castle Dr, Dunfermline, UK

HIGHLIGHTS

- Filtration performance was assessed using different data driven diagnostic methods.
- Filtration was effectively modelled using operationally relevant predictor variables.
- The CART algorithm was an effective tool for the diagnosis of operational filtration performance.

ARTICLE INFO

Article history:

Received 9 October 2016

Received in revised form 9 December 2016

Accepted 11 December 2016

Available online 16 December 2016

Keywords:

Filtration

CART

Turbidity

Fault diagnosis

ABSTRACT

Rapid gravity filters, the final particulate barrier in many water treatment systems, are typically monitored using on-line turbidity, flow and head loss instrumentation. Current metrics for assessing filtration performance from on-line turbidity data were critically assessed and observed not to effectively and consistently summarise the important properties of a turbidity distribution and the associated water quality risk. In the absence of a consistent risk function for turbidity in treated water, using on-line turbidity as an indicative rather than a quantitative variable appears to be more practical. Best practice suggests that filtered water turbidity should be maintained below 0.1 NTU, at higher turbidity we can be less confident of an effective particle and pathogen barrier. Based on this simple distinction filtration performance has been described in terms of reliability and resilience by characterising the likelihood, frequency and duration of turbidity spikes greater than 0.1 NTU. This view of filtration performance is then used to frame operational diagnosis of unsatisfactory performance in terms of a machine learning classification problem. Through calculation of operationally relevant predictor variables and application of the Classification and Regression Tree (CART) algorithm the conditions associated with the greatest risk of poor filtration performance can be effectively modelled and communicated in operational terms. This provides a method for an evidence based decision support which can be used to efficiently manage individual pathogen barriers in a multi-barrier system.

© 2016 The Author(s). Published by Elsevier B.V. This is an open access article under the CC BY license (<http://creativecommons.org/licenses/by/4.0/>).

1. Introduction

Rapid gravity filters provide the final barrier to particulates in most large municipal water supply systems. Public health risk arising from large water supply systems is primarily associated with short duration contamination or challenge events, such as those associated with extreme weather events, which are poorly captured by regulatory sampling programmes [1]. Breakthrough and transient periods of high turbidity have been associated with increased concentrations of oocysts, suspended solids and spore forming bacteria in distribution systems [2,3]. In addition, turbid-

ity is widely interpreted and assumed to indicate removal performance of water-borne environmental pathogens [4,5]. Therefore, on-line turbidity meters provide a record to evidence filtration performance with a degree of granularity far greater than can be achieved by regulatory sampling.

Turbidity quantifies the extent to which suspended particles scatter light subject to their concentration, size and colour [6]. As an optical property, turbidity is not a direct health risk but has been associated with the presence of bacteria, the shielding of microorganisms from disinfection, causing additional chlorine demand, increasing disinfection-by-product (DBP) formation and promoting biological growth in distribution [7,8]. In the UK, the prescribed value for turbidity is 4 Nephelometric Turbidity Units (NTU) at the customer's tap with an indicative limit of 1 NTU for water leav-

* Corresponding author.

E-mail address: p.jarvis@cranfield.ac.uk (P. Jarvis).

ing the treatment works [9]. The World Health Organisation suggests that prior to chlorination large municipal supplies should average below 0.2 NTU and not exceed 0.5 NTU [10]. A best practice target of 0.1 NTU has been proposed to limit the risk of pathogen passage [11]. Water utilities aim to maintain low filtered water turbidity in order to minimise risk of bacteriological failure, reduce the cost of additional chemical dosing and lower DBP formation [12]. Though limitations to the sensitivity of turbidity have been observed in comparison to particle count monitoring its simplicity, reliability and economy ensure that turbidity remains the most widely used parameter for monitoring filter performance [12,13].

Visualisation of turbidity records is routinely used to assess and diagnose performance [14]. Typically, efforts by operators and scientists to monitor and improve the performance of filtration processes in terms of turbidity have used averages, percentile statistics, or compliance with a target value over various periods [12,15–17]. To aid consistent and objective management, investigators and practitioners have developed turbidity robustness indices (TRIs) to improve understanding of performance [11,18,19]. However, these metrics have not routinely been applied in practice. One of the aims of the research was to assess the suitability and reliability of these indices. Alternative approaches to performance assessment can be based around the best practice target of 0.1 NTU [11]. Performance can then be described in terms of the likelihood, frequency, and duration of quality target breaches. Such an approach, allows the application of basic reliability engineering metrics such as the mean time between failures (MTBF) and the mean time to recovery (MTTR) which can be applied to indicate reliability and resilience.

Once detected, a process fault is typically diagnosed by one of the following: from reference to prior information in quantitative or qualitative models of the process; by using historical data; or by combining more than one approach [20]. Purely quantitative modelling approaches to diagnosis of filtration performance are impractical because the underlying complex non-linear particle separation process is not accurately described by theory and measurement. Phenomenological and theoretical filtration models often rely on measurements which are not routinely collected in full scale water treatment [21,22]. Turbidity, for example, is not a quantitative measurement. The formalisation of qualitative knowledge into models is challenged by behavioural complexity of the process, inflexibility to new conditions and the generation of spurious diagnosis [23]. Process history based methods have been broadly categorised as quantitative or qualitative depending upon the method by which historical data is transformed and applied within the diagnostic system [24]. Current guidance suggests a form of manual qualitative trend analysis for rapid gravity filter fault diagnosis. This requires the time-consuming manual inspection and interpretation of filter profiles in order to identify potential issues and confirmation with further physical inspections and process investigation [15]. This investigation proposes a quantitative method to identify key operational issues associated with elevated filtrate turbidity, applicable over extended periods to provide easily interpretable diagnostic models for rapid gravity filtration operation and maintenance decisions. Such models can guide investigations reducing the time and financial and environmental cost incurred.

Treatment operators and managers need efficient, effective, robust and justifiable tools and methods for the aggregation and interpretation of large volumes of filter monitoring data into useful information from which evidence based decisions can be made. Using a turbidity target, such as the best-practice level of 0.1 NTU, we can frame the analysis of control system data as a classification problem whereby we identify the conditions associated with greater likelihood of high filtrate turbidity. Classification is a common task in machine learning and can be achieved by numer-

ous methods which can broadly be categorised into; linear, Bayesian, tree-based, clustering, neural-network and ensemble approaches. Broadly, linear methods such as logistic regression, identify and optimise a linear function to classify between one or more categories and Bayesian methods apply Bayes' rule. Tree based methods use recursive binary splitting of the feature space to fit a stepwise function. Clustering methods typically classify based on the Cartesian distance. Neural networks mimic the function of the human brain by optimising a collection of weightings and transfer functions (neurons) to return the most effective classifying function from a given architecture. Ensemble methods combine the results of many simple classification models to improve overall performance. Classification trees have been chosen for this application based on their primary virtue which is interpretability. This is key for the efficient and successful retrospective implementation of such a decision support tool for operators and managers facilitating more effective management of individual pathogen barriers. Further advantages of the classification tree methods are that they work effectively using discrete and continuous variables of any distribution and are insensitive to outliers [25].

The primary criticisms of classification trees are comparatively poor accuracy, a tendency to over-fit, instability and poor capture of additive structure. The objective of this investigation was to develop workable methods which can be applied to improve operational and preventative maintenance decision making on water treatment assets and for this reason interpretability trumps accuracy in this application. Though it is likely that alternative classification methods may produce better classification accuracy, the generation of the classification tree models allows far more broadly accessible communication and sense checking of the diagnosis. The tendency of classification trees to over-fit the data can be mitigated by appropriately using k-fold cross validation to estimate the extent of model pruning required. The problem that a small change in the data can cause a large change in the model and that similar splits often appear on multiple branches is inherent in the binary splitting algorithm and are the trade-off for the simplicity of interpretation [25].

Though classification trees have been implemented by numerous algorithms the two most popular methods are the classification and regression tree approach (CART) and the C4.5 and C5.0 algorithms [26]. The main distinctions between the implementation of these methods are the use of different functions to inform the split location, alternative pruning procedures, the possibility for multiway splits on categorical predictors and the potential for conversion to rules. CART has been widely applied and popular due to its accessibility and ease of interpretation when applied to non-linear processes [25]. CART has been applied to understanding and managing water contamination events and mechanisms [27,28]. Through recursive partitioning of explanatory variables, the conditions associated with an outcome of interest can be simplified and presented in an interpretable tree format using the classification and regression tree (CART) algorithm [29]. The CART algorithm is used in this study to produce interpretable models describing the operational conditions associated with the occurrence of elevated filtrate turbidity.

The aims of this paper were therefore to develop intelligent, data-driven decision support systems by assessing and developing existing performance metrics for summarising the performance of filtration processes in terms of turbidity and utilising other typical sources of data to identify the likely causes.

2. Materials and methods

Data was extracted from the control system at a water treatment plant in Scotland treating a mix of two upland surface water

sources by coagulation, flocculation, dissolved air flotation, rapid gravity filtration and chlorination. Data for the whole of 2015 describing turbidity, flow, level and head-loss for four filters as well as raw water temperature and clarified water turbidity data was extracted at 30 s intervals. Data handling and analysis was performed using a PostgreSQL 9.4 database, R 3.2.0, and RStudio [30–32]. The key R packages used were lubridate [33], ggplot2 [34], dplyr [35], RPostgreSQL [36], caret [37] and rpart [38].

Data for individual filters were split into in-service and out of service periods and individual filter runs were delineated based on threshold values for flow, level and head loss. Prior to analysis the turbidity time series at 30 s intervals were cleaned to remove specific artefacts. High turbidity values likely associated with trapped bubbles or detachment of biofilm within the sample line were removed then a hampel filter was applied over the natural log transformed turbidity time series with a window length of 15 observations and a threshold of 3 standard deviations. This removed outliers, attributable to measurement, data collection and sampling error, from the local trend over a rolling window and replaced them with the local median value. This process removed false low and high outliers from bubbles passing through the measurement cell preventing them from influencing assessment of the frequency and duration of real turbidity spikes in the filtered water.

A number of performance statistics were applied to turbidity data in order to communicate the relative merits of different approaches. The simple descriptive statistics applied were the mean, median, standard deviation, 90th, 95th and 99th percentiles. To describe the distribution of turbidity data over a period of operation a number of turbidity robustness metrics (TRIs) have been proposed evolving from the original Eq. (1) proposed by Huck [12]

$$TRI_p = \frac{1}{2} \left[\frac{T_p}{T_{50}} + \frac{T_{50}}{T_{goal}} \right] \quad (1)$$

where

T_p = p th percentile turbidity and
 T_{goal} = targeted turbidity value

The TRI function summarises a distribution of turbidity data in a single value by taking a quotient of percentiles as a proxy for variance and right skew and the quotient of the median and a goal value as a location term then averaging these two terms. This metric has been applied to demonstrate changes in clarifier and filter performance [39,40]. Subsequent modifications to improve metric performance were proposed in Eq. (2) which involved weighting

the terms of the original metric to provide outcomes more consistent with expectations and an algorithm was applied to assign the weights [18]. A further investigation simplified the allocation of weighting based on the time below the turbidity goal Eq. (3) [19].

$$TRI_{90D} = \left[A_1 \frac{T_{90}}{T_{50}} + A_2 \frac{T_{50}}{T_{goal}} \right]$$

where

if $W \leq N$ & $T_{90}/T_{50} \leq T_{50}/T_{goal}$ $A_1 = 0.9, A_2 = 0.1$ else
 if $W \leq N$ & $T_{90}/T_{50} > T_{50}/T_{goal}$ $A_1 = 0.1, A_2 = 0.9$ else
 if $W > N$ & $T_{90}/T_{50} \leq T_{50}/T_{goal}$ $A_1 = 0.1, A_2 = 0.9$ else
 if $W > N$ & $T_{90}/T_{50} > T_{50}/T_{goal}$ $A_1 = 0.9, A_2 = 0.1$

and

$N = 0.5$ and

$$W = \left(\frac{T_{50}}{T_{goal}} + \frac{T_{60}}{T_{goal}} + \frac{T_{70}}{T_{goal}} + \frac{T_{80}}{T_{goal}} + \frac{T_{90}}{T_{goal}} \right) * 10 \quad (2)$$

$$TRI_p = \left[\left(1 - \frac{G\%}{100} \right) * \frac{T_p}{T_{50}} \right] + \left[\frac{T_{50}}{T_{goal}} * \frac{G\%}{100} \right] \quad (3)$$

where

$G\%$ = time below turbidity goal

A new approach to managing filtration can be developed from a binary view of performance based on compliance with 0.1 NTU. The simple discrete failure rate aggregates two distinct aspects of performance, reliability and resilience. Though limited, common metrics can be used to summarise these different aspects of performance. Reliability, or the frequency of failure events over a given period, is often characterised using the mean time between failures Eq. (4). Resilience, the time that a system takes to return to acceptable performance when a failure event does occur, can be described using the mean time to recovery Eq. (5).

$$MTBF = \frac{\sum_{i=0}^{i=n} (\text{start of spike}_i - \text{end of spike}_{i-1})}{n} \quad (4)$$

$$MTTR = \frac{\sum_{i=0}^{i=n} (\text{end of spike}_i - \text{start of spike}_i)}{n} \quad (5)$$

In order to facilitate differential diagnosis of operational filtration issues a number of relevant variables were derived from the time-stamped observations from other signals (see Table 1). Head loss was normalised against a standardised flow of 50 l/s at 10 °C in order to provide a more useful comparison of media condition using

Table 1
 Predictive features for CART diagnostic model.

Explanatory variable	Description
HoursInRun	The time in hours elapsed since start of filter run allows distinction between early and late run filtration issues
BankFlowTrend	A two-hour average flow to filter bank (l/s) captures the hydraulic loading to the whole system
MaxBankFlowIncrease	The maximum filter bank flow (l/s) increase over 30 min during previous 90 min, captures increases in hydraulic loading to the whole system
BankFlowProportion	The proportion of total flow to bank treated by an individual filter indicates if the distribution of flow between filters is associated with performance
FlowShock	The difference between the instantaneous rate of flow and the average over the run (l/s) captures periods of additional hydraulic loading such as those during washing of another filter
ClarifiedTurbidityTrend	An average clarified turbidity (NTU) since the start of the run provides an indication of the solids loading
ClarifiedTurbiditySpike	The maximum difference between 30-min average clarified turbidity and “ClarifiedTurbidityTrend” experienced since the start of the run to capture shock solids loading
temp	Temperature is known to affect particle separation and filter washing (measured at raw water inlet Celsius)
CleanBedHeadLoss	Head loss at the start of the run normalised for flow and temperature as indicated by the intercept of the head loss model Eq. (6)
ScaledCleanBedHeadLoss	The within filter z score of “CleanBedHeadLoss” used to capture variation in post-wash media condition rather than differences between filters
HeadlossCoefficient1	The growth m/m ³ of normalised head loss over the course of the filter run indicates the rate at which hydraulic resistance accumulates within the bed
HeadlossCoefficient2	The change in rate of hydraulic resistance accumulation with volume filtered

the method described in [15]. As head loss is strongly correlated with the number of hours in service this effect was removed by fitting a second-order linear regression model to describe head loss within each filter run in terms of the volume of water filtered since the last wash Eq. (6). Prior to fitting the model, outlying head-loss observations more than 2 standard deviations from the within-run mean were removed. Average r-squared values for the head-loss models in the four filters were 0.98, 0.96, 0.93 and 0.99 in filters A–D respectively. The coefficients for these head loss models were then extracted and used as explanatory features in the diagnostic models. The model intercept, used to estimate normalised clean-bed head loss, was converted to a z-score within the group of runs for each filter for use in diagnostic modelling of multiple filters. The slope coefficients were used to characterise head-loss accumulation and change in rate during the run.

$$\text{Normalised Head Loss} = \beta_0 + \beta_1 v + \beta_2 v^2 + \varepsilon \quad (6)$$

where

v = volume filtered since wash, ε = error.

Useful information from the potential explanatory variables was then extracted using a classification algorithm. An implementation of the CART algorithm was applied to build simple explanatory classification models of the conditions associated with “HIGH” > 0.1 NTU and “OK” \leq 0.1 NTU filtrate [29]. CART applies recursive partitioning to split a multi-dimensional predictor space into regions with an assigned classification in the response variable. The data is split on the point on an explanatory variable which minimises “risk” calculated from the loss adjusted Gini purity (a measure of class imbalance) in the resulting two groups. Due to the underlying public health objective of water treatment false negative classifications are more undesirable than false positives. Therefore, a loss matrix was applied during model training which weighted the penalty of false negatives by a factor of 10. In order to simply and effectively describe the underlying data the size of the classification model needs to be restricted. The extent to which the model is pruned is determined by the complexity parameter which is the cost assigned to each additional terminal node. The smallest tree that minimises the sum of the loss adjusted Gini purity and complexity cost is then selected. The value of the complexity parameter was tuned using 10-fold cross validation using the area under the receiver operating characteristic curve to assess model fit and select the best value. The performance of the final model was tested by applying the model to 20% of the data

retained for testing by comparing the predicted and observed classes. The CART algorithm was used to review a period of filter operation and characterise the occurrence of elevated turbidity in order to aid understanding of past filter performance. A classification tree model was trained for each filter each week where the probability of exceeding 0.1 NTU was greater than 1 in 1000 which is equivalent to a single 30 s measurement in 20.16 h. Failure rates below this level are of less concern for public health and less predictable as error in measurement and data systems is likely to contribute a greater proportion of failing measurements as the total failure rate decreases. The approach was then tested again over each monthly period looking at all of the filters in the bank in order to explore more general operational issues common between filters over an extended period.

3. Results

3.1. Filtration performance data

An overview of the turbidity data for the four filters assessed is presented in time series and cumulative distribution format (Fig. 1). The time series indicates higher turbidity and therefore worse performance at the start and end of the year. The cumulative distribution indicates that filters A and D are the best and worst performers respectively. To provide a more detailed view for comparison data for every 10th week was selected and plotted both as a time series (Fig. 2) and a cumulative distribution (Fig. 3). In week 1 it can be seen that turbidity from filters B–D deteriorates rapidly during the filter run and exhibits several turbidity spikes throughout the run with the cumulative distribution of turbidity for filter D clearly indicating the worst performance. Improved performance can be seen through weeks 11 and 21 with lower turbidity. By week 31 turbidity spiking is only evident from filter C. No large turbidity spikes are evident during week 41. During week 51 turbidity appears to deteriorate during the run for filter D. These examples illustrate variation in turbidity profiles and distributions in filters with inconsistent performance.

3.2. Assessment of performance metrics

A number of summary statistics including mean, median, standard deviation, 90th, 95th and 99th percentiles, were calculated using the filtrate turbidity data for each week of the 2015 period

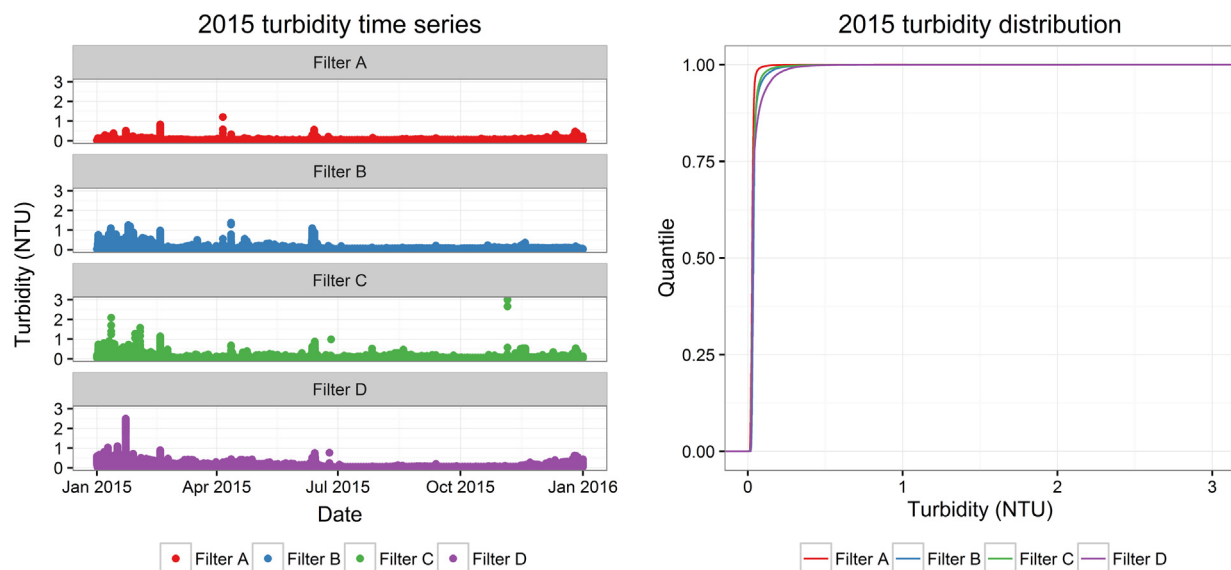


Fig. 1. Filtrate turbidity data for 2015 plotted as a time series and cumulative distribution.



Fig. 2. Turbidity time series for weeks selected to demonstrate variation in filter performance.

(Fig. 4). Similarly, values returned by the TRID and TRIJ metrics Eqs. (2) and (3) at the 90th, 95th and 99th percentile variants for the same data have been compared (Fig. 4). Superficially there is a broad consensus in the performance metrics which show typically poor performance at the start of the year, which improves mid-year before deteriorating at the end of the year. However, Spearman's rank correlations between metric scores illustrate the varying levels of agreement (Table 2). The TRIJ metric at all percentiles shows greater agreement with the mean than the TRID. However, the standard deviation is more strongly associated with the TRID than the TRIJ. Though both the TRIJ and TRID show a strong relationship between the values returned for different percentiles, greater consistency between metrics applied at different percentiles is shown by the TRIJ metric than the TRID. Only moderate correlations between TRID and TRIJ scores are apparent indicating diverging perspectives on filtration performance. Using the same data, the failure rate, mean time between failure and mean time to recovery Eqs. (3) and (4) based on a filter achieving the best practice target of 0.1 NTU are shown in Fig. 5. The failure rate shows a pattern similar to the traditional performance metrics with performance improving during the first part of the year before declining slightly at the end. The number of hours that the filter operates, on average, before exceeding 0.1 NTU clearly shows variation in the reliability of different filters (Fig. 5 B). Filter A is shown to be most consistently reliable and filter D is shown to have periods of both good and poor reliability. For much of the year, however, filters B and C exhibit a turbidity spike greater than 0.1 NTU at least once every two days. The average duration in hours of turbidity spikes, illustrative of process resilience, indicates that turbidity spikes are typically less than half an hour in duration

(Fig. 5 C). However, this is not the case for filter D at the start of the year or occasionally in filter A which both exhibit periods above 0.1 NTU lasting over an hour. The expression of performance in terms of rates and time is more intuitively comparable than values derived from weighted quotients of percentiles of the turbidity distribution.

3.3. Filter performance diagnosis

Diagnosis of the cause of poor filtration performance is key to managing and reducing water quality risk. In order to demonstrate the effectiveness of classification trees an example of a weekly model for Filter D Week 21 is shown in Fig. 6. Each circular node describes a split in the data describing filter operation. The first split (FlowShock >0.193) divides observations into those which are associated with a hydraulic shock, whereby the instantaneous flow rate was greater than 1.193 times the mean flow for the filter over the run. It was this point that most effectively split the turbidity observations in the training data into those which were greater than or less than 0.1 NTU. Each rectangular leaf node describes the performance of the filter given the particular conditions as described by the nodes above. Three lines of text in the leaf node describe the probability of a "HIGH" (>0.1 NTU) turbidity reading, the complimentary probability of "OK" turbidity and the overall probability, during the period of interest, that those conditions would be observed. The outputs from the developed models showed that they provided a highly accurate description of the conditions associated with correct classification for >75% of observations in the worst performing model and average accuracy between 94% and 99% depending on the filter (Table 3). Average

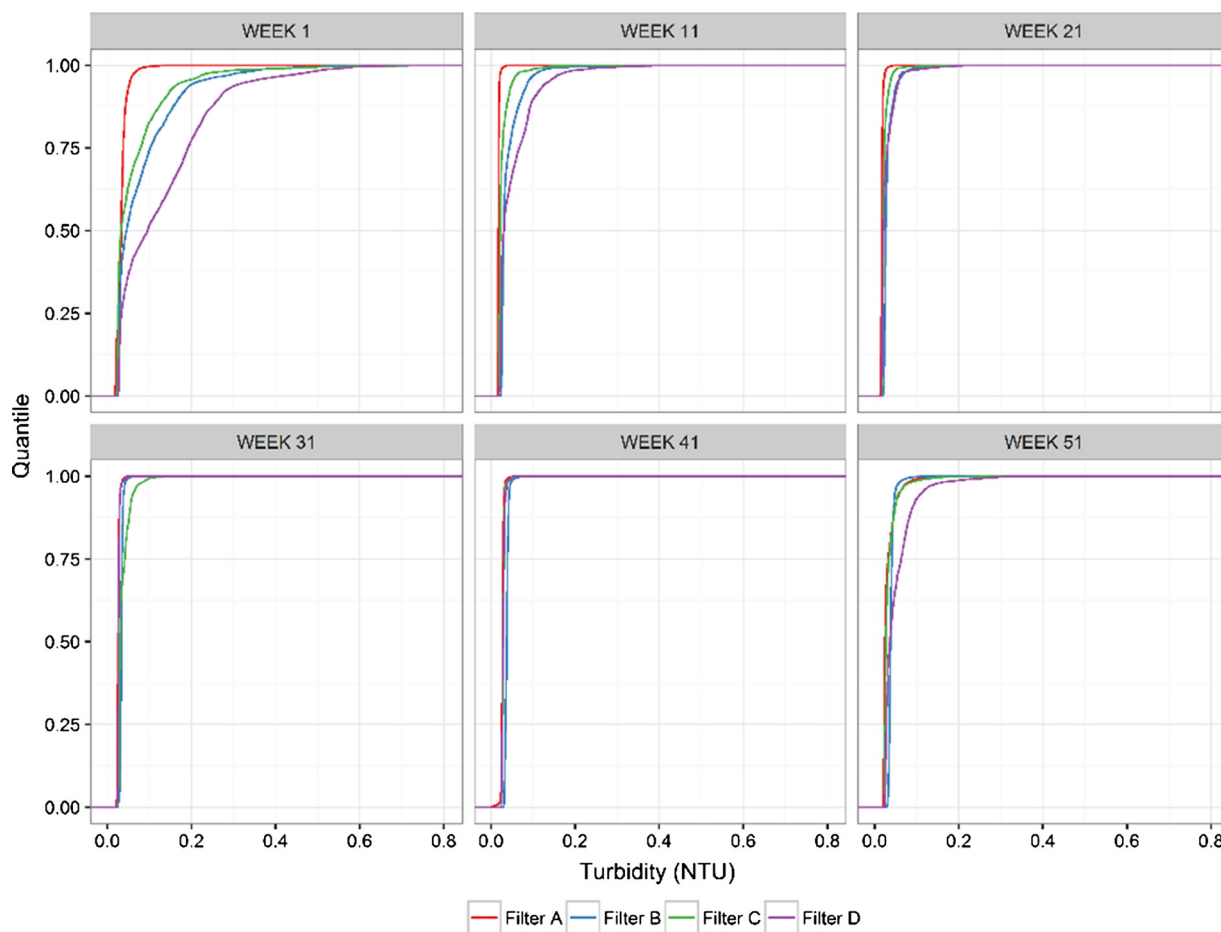


Fig. 3. Cumulative turbidity distributions for weeks selected to demonstrate variation in filter performance.

true positive rates for high turbidity values were greater than 91% for all filters.

The classification tree approach is not limited to informing on week to week operation of individual filters. An additional categorical variable indicating the specific filter was added to the model and clean bed head loss was scaled for each of the filters using a z score.

We can see that the monthly models typically have good accuracy >0.75 , however model sensitivity (true positive rate) was lower in some of the months that experienced better filter performance (Table 4). In July only 55% of high observations were explained by the model however, the failure rate was only 0.1%. The classification tree model for the month of January is plotted to provide an example (Fig. 7). It shows that those filters treating more than 24% of the flow to the bank had a 0.48 probability of producing “HIGH” turbidity water after 15 h, indicating that earlier washing was required at this hydraulic loading. There was a 0.28 probability of high turbidity in the first hour and 20 min, suggesting an undesirably long ripening period. Between 1.3 and 15 h into a run filter D had a 0.19 probability of producing “HIGH” turbidity water if it had experienced a spike in clarified water turbidity of greater than 0.12 NTU above trend. Classification trees such as those demonstrated can effectively identify and clearly communicate the conditions associated with poor filtration performance.

4. Discussion

The cyclic operation and dynamic characteristics of filtration typically produce a fluctuating turbidity trend from which a rela-

tive comparison of performance may not be visually intuitive (Figs. 1 and 2). To aid clearer comparison, turbidity data are often plotted as a cumulative distribution, though information is lost describing the time and operational context (Fig. 1). The underlying processes giving rise to filtrate turbidity vary as do properties of the resultant distributions (Figs. 2 and 3). An appropriate method for the quantification of performance through the aggregation of this data is important for the effective management of the treatment process which requires the effective comparison of performance over time and between filters in order to direct preventative maintenance.

4.1. Performance assessment

Though widely used, the average turbidity (mean or median) is not the most appropriate property of the distribution upon which to compare filter performance (Fig. 4A, B). This is because unless a filter is suffering acute and prolonged periods of poor performance, average turbidity is likely to be below 0.2 NTU. Without visibility of the underlying distribution it is not clear if differences in mean turbidity arise from turbidity spikes of concern or bias at the lower end of the measurement range. For example, average turbidity of 0.05 NTU from one system or period of operation cannot consistently be assumed to represent lower risk than turbidity of 0.07 NTU from another. The insensitivity of the mean and median statistics are demonstrated when comparing the performance of filters B and C during weeks 31 and 41 where both statistics fail to capture the significant spiking which occurs in the filtrate turbidity of filter C during week 31 (Figs. 2 and 3). The median and

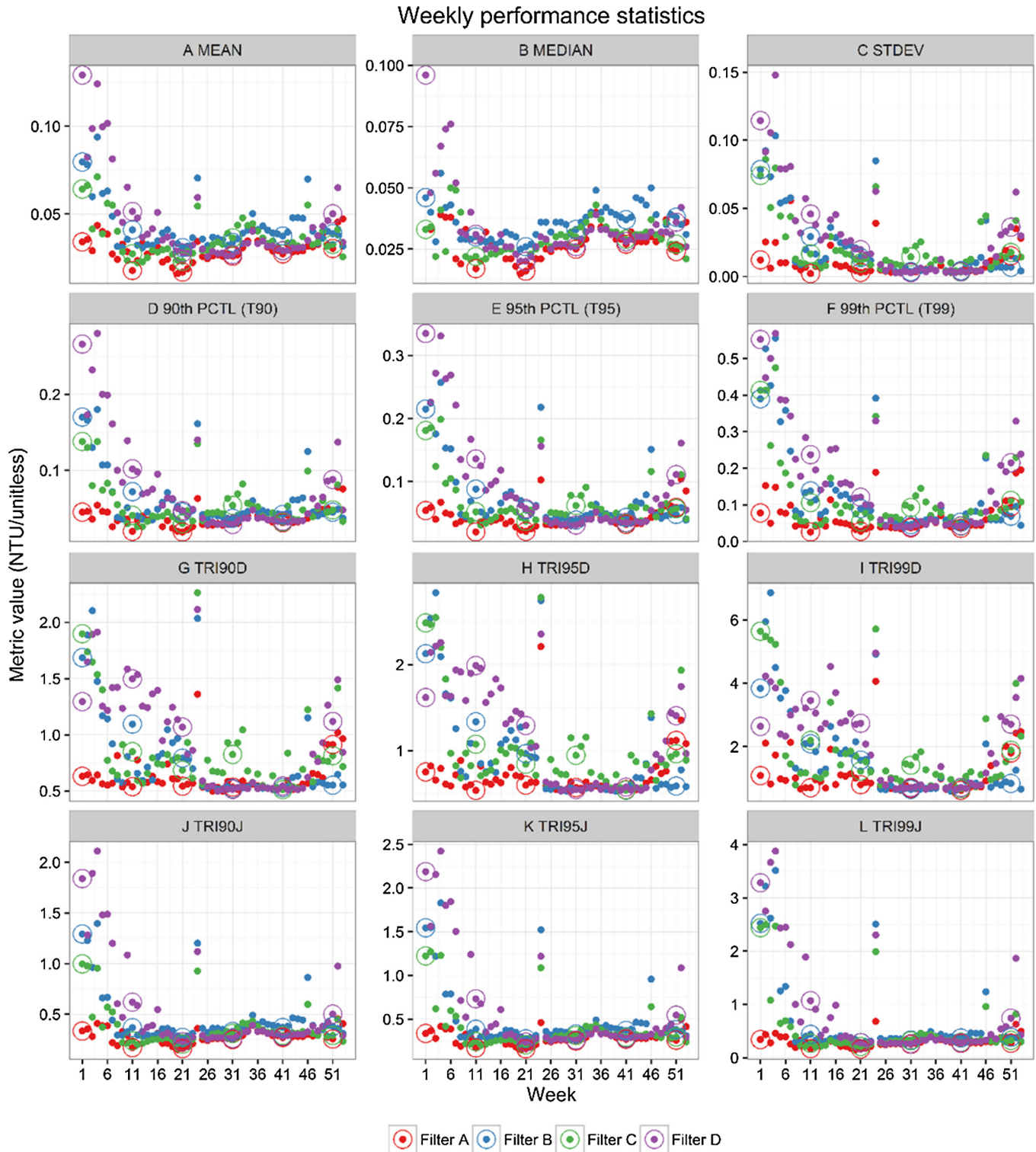


Fig. 4. Values returned by performance statistics. The points corresponding to the six selected weeks are circled.

mean are sensitive, however, to the comparatively higher turbidity recorded during normal operation in filter B which, with the limitations of the measurement, hold little useful information and are likely to arise from measurement error.

The standard deviation of turbidity (Fig. 4C) is generally effective and appropriate for comparing the variation in the right tailed distributions of filtrate turbidity during inconsistent performance. However, the statistic may not always appropriately compare dis-

tributions with varying kurtosis. It is common to select a high percentile value with which to compare performance (Fig. 4D–F). As turbidity time series exhibit inconsistent skewness and kurtosis between groups and over time, comparison of a single percentile value will not be a consistent basis for comparison (Fig. 3). Two distributions, one with a short fat tail and another with a long thin tail may return an equal 95th percentile but reflect quite different turbidity risk. A process may completely fail for 4% of the period

Table 2
Spearman's rank correlations between performance statistics.

	A MEAN	B MEDIAN	C STDEV	D 90th PCTL (T90)	E 95th PCTL (T95)	F 99th PCTL (T99)	G TRI90D	H TRI95D	I TRI99D	J TRI90J	K TRI95J
A MEAN	1.00	0.81	0.63	0.90	0.85	0.74	0.52	0.49	0.46	0.97	0.98
B MEDIAN	0.81	1.00	0.20	0.55	0.47	0.33	0.03	−0.01	−0.03	0.85	0.82
C STDEV	0.63	0.20	1.00	0.82	0.89	0.96	0.92	0.93	0.94	0.51	0.55
D 90th PCTL (T90)	0.90	0.55	0.82	1.00	0.98	0.88	0.79	0.75	0.70	0.81	0.83
E 95th PCTL (T95)	0.85	0.47	0.89	0.98	1.00	0.94	0.85	0.84	0.79	0.75	0.77
F 99th PCTL (T99)	0.74	0.33	0.96	0.88	0.94	1.00	0.86	0.87	0.91	0.63	0.67
G TRI90D	0.52	0.03	0.92	0.79	0.85	0.86	1.00	0.98	0.92	0.39	0.42
H TRI95D	0.49	−0.01	0.93	0.75	0.84	0.87	0.98	1.00	0.95	0.36	0.40
I TRI99D	0.46	−0.03	0.94	0.70	0.79	0.91	0.92	0.95	1.00	0.34	0.38
J TRI90J	0.97	0.85	0.51	0.81	0.75	0.63	0.39	0.36	0.34	1.00	1.00
K TRI95J	0.98	0.82	0.55	0.83	0.77	0.67	0.42	0.40	0.38	1.00	1.00
L TRI99J	0.97	0.74	0.66	0.88	0.84	0.77	0.53	0.50	0.51	0.96	0.97

Alternative weekly performance statistics

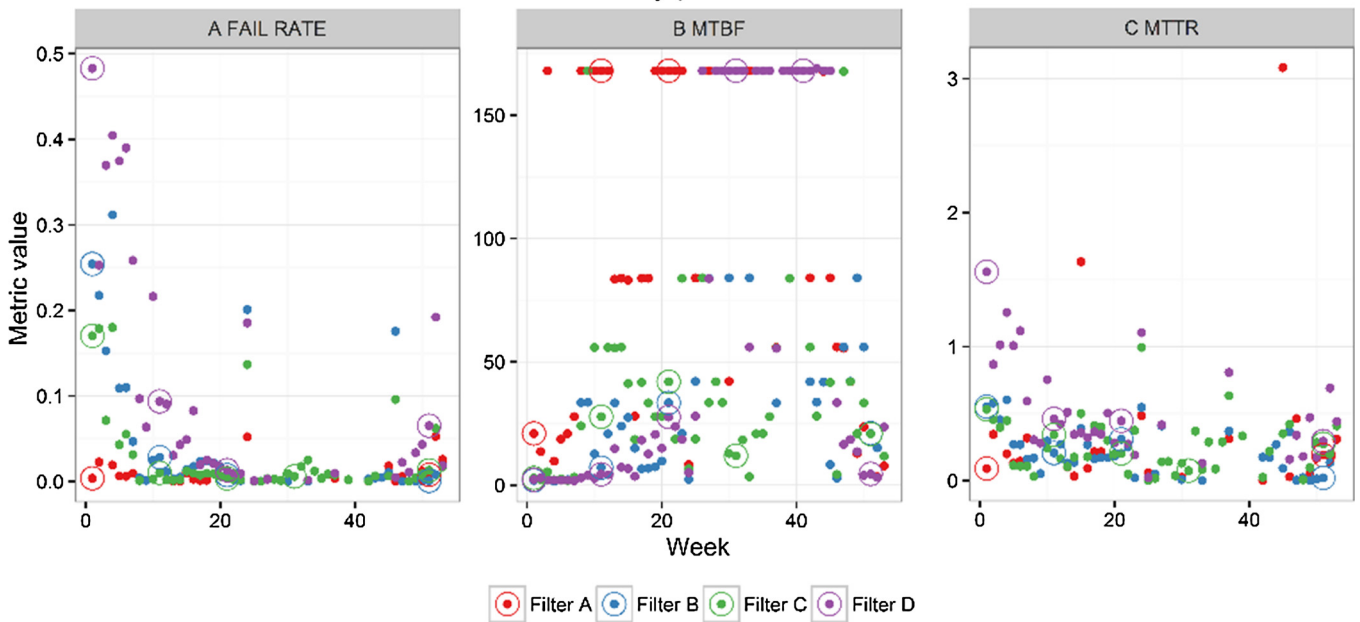


Fig. 5. Performance assessment based on a binary classification of turbidity.

without impacting on the performance as measured by the 95th percentile. The choice of a high percentile (T90–T99) affects the relative assessment of performance between filters B and C during week 1 (Fig. 4D–F). The 90th and 95th percentiles for filter B are greater than those of filter C, however, the 99th percentile for filter C is greater than filter B. There remains no clear empirical or theoretical link that supports the assessment of overall performance on the basis of a single percentile value.

Turbidity robustness indices have developed from the TRIE Eq. (1) with additional terms and weighting procedures but fall short of addressing distortions arising from variation in tail shape. The relative performance of filters as described by the TRID [18] and TRIJ [19] metrics are illustrated in Fig. 4(G–L). The first term of the TRI metrics takes the quotient of two percentiles (Eqs. (1–3)) in a manner analogous to the uniformity coefficient applied to filter media [15]. Such an approach may function when comparing similarly shaped distributions but is not reliable when the skewness and kurtosis of the underlying distributions are inconsistent. As a lower median turbidity (denominator) will result in a larger quotient there is an unjustified penalty for better average turbidity

given the same high percentile value. The weakness of the TRID in this regard is clear when comparing week 1 (Fig. 4G–I) where filter D has a TRI90D less than filters B and C which is clearly counter intuitive upon examination of the time series and distributions (Figs. 2 and 3). The second term common to the TRI metrics takes the median and divides it by the goal turbidity, typically between 0.1 and 0.3 NTU. Assuming a consistent target turbidity this term does not serve to usefully differentiate performance any more than taking the median. The differentiating elements of the original TRIE metric could therefore be simplified to $T90/T50 + T50$ which, given the limitations of using percentiles, is unlikely to be the best approach for comparing performance. Though the additional procedures for weighting terms implemented in the TRID metric remove some cases where nonsense TRIE values would be returned, the examples identified demonstrate that the method is fallible. Though the TRIJ introduces a simpler and more stable method for weighting terms, the use of arbitrary percentile values continues to exhibit an influence on the relative assessment of performance between filters with turbidity distributions of different shape (Fig. 4J–L).

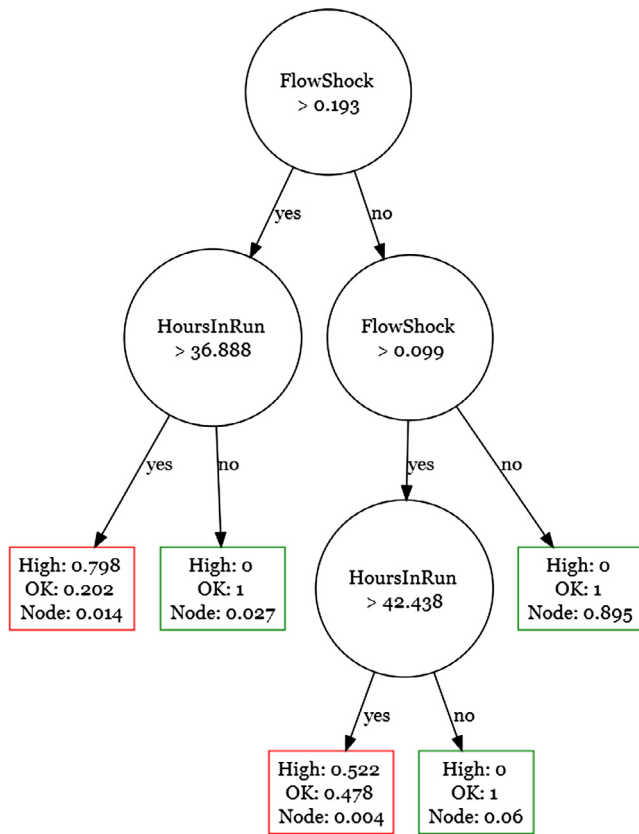


Fig. 6. Example classification tree model for Filter D Week 21.

A more appropriate approach is to apply best practice guidance which indicates that turbidity greater than 0.1 NTU is indicative of a filtration performance issue [11]. Breaching this limit can be considered as “failure”, such a binary approach is appropriate given uncertainties in the relationship between turbidity and water quality risk allowing a simple and effective way to incorporate performance comparison on the basis of time. The failure rate against a goal of 0.1 NTU is a good metric for filtration performance as it is understandable, comparable, insensitive to measurement error and easily applied (Fig. 5 A). For example, in week 1 filter D spent almost twice as much time over 0.1 NTU than filter B. The reliability of a filtration process can be compared by contrasting the average duration of acceptable performance between turbidity spikes (Eq. (4)). The performance of filters spiking more frequently can be described as being less reliable. The MTBF shows that filter A typically appears to be more reliable than the other filters throughout the year with a longer average interval between turbidity spikes (Fig. 5 B). Poor performance may be a result of frequent spikes in filtrate turbidity or less frequent but more extended periods of poor performance, the causes of which are likely to be functionally different and therefore of interest in the management of the process. Insight, in this regard, can be gained by examining the interval between turbidity events. However, it should be

Table 4
Summary of monthly models for individual filters performance.

Month	>0.1 NTU%	Accuracy	Sensitivity	Specificity
Jan	15.00	0.75	0.96	0.70
Feb	7.10	0.85	0.81	0.86
Mar	2.60	0.94	0.93	0.94
Apr	1.50	0.96	0.74	0.96
May	0.80	0.99	0.84	0.99
Jun	2.90	0.95	0.87	0.96
Jul	0.10	1.00	0.55	1.00
Aug	0.30	1.00	0.89	1.00
Sep	0.20	0.99	0.95	0.99
Nov	1.70	0.98	0.85	0.98
Dec	2.40	0.92	0.81	0.92

acknowledged that as high turbidity events are likely to cluster, the mean time between failures is an indicator only. The resilience of the performance of a filter can be compared by contrasting the average duration of turbidity spikes which are observed (Eq. (5)). Filters which on average return to acceptable performance in a shorter time can be considered to be more resilient. Filter D can be seen to be the least resilient early in the year with turbidity spikes lasting on average over an hour (Fig. 5C).

The alternative measures of filtration performance described offer a sensible and intuitive approach to characterising the aspects of performance which are effectively measured using turbidity. The main advantage of these approaches is that they do not depend on consistent skewness of the turbidity distribution to be comparable. Furthermore, when applying the failure rate, MTBF and MTTR there is no reliance on an implicit assumption that risk is a consistent linear function of turbidity. There is merely an assumption that turbidity above 0.1 NTU is consistently indicative of greater risk than turbidity less than 0.1 NTU. Assessment of filter performance on the basis of turbidity could be further improved by the effective definition of a risk function for turbidity.

4.2. Diagnosis

In order to effectively manage filtration performance, an understanding of the causes of poor performance is required. Diagnosis of filtration issues is traditionally achieved through interpretation of turbidity time series and normalised starting head loss. Approaches to the interpretation of turbidity trends over the period of a filter run are well described and have been used to characterise a number of filtration issues [15]. However, these methods are manual, time consuming and subjective which can restrict their application. Through automation of the analysis, such interpretation can be applied much more broadly to understanding marginal treatment performance concerns. Other researchers have observed that by addressing such performance issues in individual treatment stages with preventative maintenance the likelihood of acute compound treatment failures can be reduced [20]. In this research the assessment of filtration performance as “HIGH” if > 0.1 or “OK” if ≤ 0.1 NTU facilitates the framing of diagnosis of these issues as a machine learning classification problem, where other sources of process data are used to build explanatory models. The CART algorithm allows the training of simple and interpretable

Table 3
Summary of weekly models for individual filters performance.

Filter	Count (weeks)	Accuracy (min, ave, max)	Sensitivity (min, ave, max)	Specificity (min, ave, max)
Filter A	18	0.91, 0.99, 1	0.74, 0.93, 1	0.91, 0.99, 1
Filter B	32	0.8, 0.96, 1	0.47, 0.91, 1	0.75, 0.95, 1
Filter C	42	0.76, 0.97, 1	0.56, 0.91, 1	0.71, 0.97, 1
Filter D	35	0.81, 0.94, 1	0.81, 0.96, 1	0.78, 0.92, 1

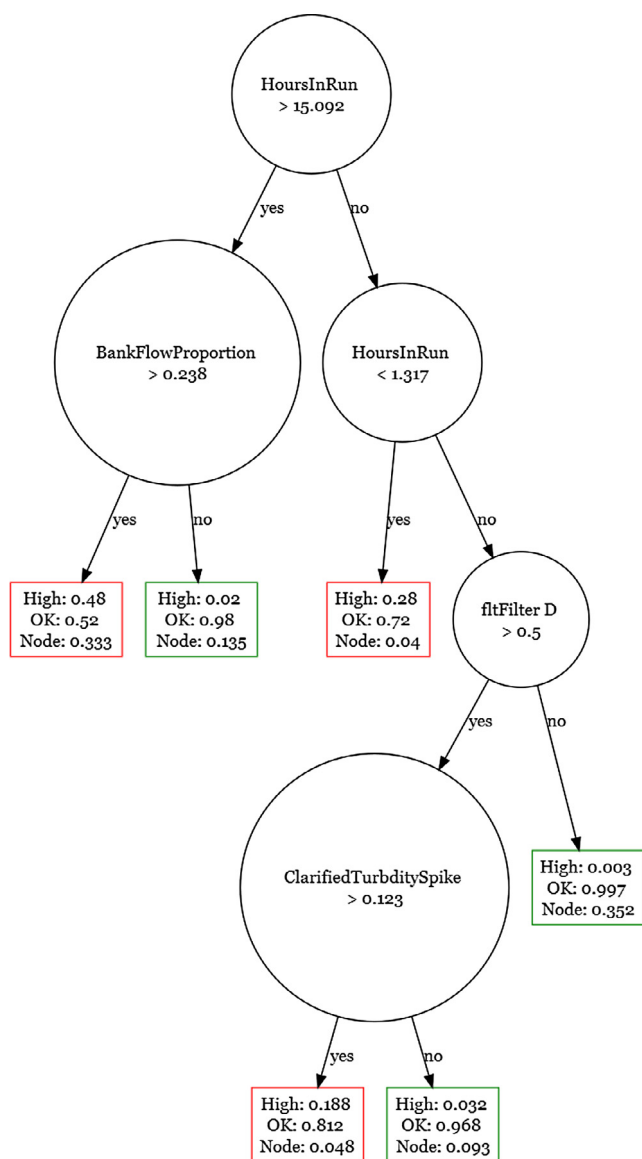


Fig. 7. Example classification tree model filter bank in January 2015.

classification tree models which effectively describe the conditions which are associated with greater risk of poor filtration performance. These models can be readily used to review the operation and control of filtration processes. The classification and regression tree algorithm provides an easily interpretable output for non-linear processes are affected by outlying observations which have been shown to represent a challenge for linear diagnostic models [41,42].

The common operational causes of poor filtration performance such as hydraulic balancing, surging, ineffective backwashing, excessively long filter runs and ineffective pre-treatment are well known [15]. Explanatory features describing these issues can be calculated from typical operational monitoring signals at a WTW (Table 1). Supplying these features to the algorithm, rather than raw data trends results in more interpretable models which are readily translated into remedial actions. As an example it is evident from Fig. 6 that high turbidity from filter D during week 21 occurred with an 80% probability during times of hydraulic shock of more than 19.3% later than 36.9 h into the filter run. After 42.4 h, a smaller hydraulic shock of only 10% was associated with a 52% chance of turbidity spiking above 0.1 NTU. Flow increases are known to cause additional shear increasing the rate of detach-

ment of particles from the media, with the effect growing more pronounced later in the run [43,44]. From this it is possible to infer that filter performance could be improved at this time by improving flow distribution or shortening the filter run. The high accuracy, sensitivity (true positive rate) and specificity (true negative rate) of the models tested provides confidence that amelioration of the conditions suggested by the model are likely to improve performance (Table 3).

In January, across the filter bank, poor performance occurred in a number of circumstances (Fig. 7). Typically, there was high turbidity in the first 1.3 h of the filter run. A number of issues have been associated with extended ripening periods, these include over-washing, low solids in the clarified water, low temperature, hydraulic overloading and ineffective particle destabilisation [15,45,46]. Reducing the initial rate of filtration is a typical process intervention in such circumstances, and more modern filters typically have a run to waste facility [15]. Flow distribution to the individual filters was clearly important later in the run with those treating more flow exhibiting greater probability of breakthrough later in the run. Balancing flows to the four filters is likely to improve the performance. Filter D was more likely to produce high turbidity water during normal filter operation after the ripening period particularly in the event of a sudden turbidity loading from a clarification issue. Further investigation indicated that flows to filter D were higher than those to the other three filters making it more vulnerable to fluctuations in clarified water quality. The simple tree model shown in Fig. 7 describes conditions associated with 96% of elevated turbidity observations during January clearly identifying operational opportunities for improving performance. The monthly models were successful at describing challenge conditions for the bank of filters with accuracy and sensitivity typically over 80% consistently demonstrating the potential for useful insight for process management (Table 4).

Though the methodology discussed has been shown to identify a range of issues related to poor performance, certain types of process fault may not be apparent using this approach. For example, long-term changes to filter characteristics which occur uniformly across filters, such as media erosion which typically takes place over years are not likely to be captured. Rapid changes, such as sudden loss of media or change in backwash performance, which impact on performance should be indicated by the influence of normalised clean-bed head loss in the diagnostic model.

Other investigations focussed on other processes have developed and employed more sophisticated approaches to fault diagnosis and adaptive model based control [24,47–49]. Despite the additional capabilities of many such historical control and diagnostic systems described in the literature there remains an implementation gap. Such process history based methods by-definition are likely to be retro-fitted to existing assets and control systems. Interaction with existing proprietary control systems is awkward or costly by design. An inherently simpler white-box method as described can flexibly facilitate operators and engineers to deliver performance improvements in many distributed assets with considerably lower barriers to implementation.

5. Conclusions

Simple performance metrics which describe the likelihood, frequency and duration of turbidity spikes using compliance rate, mean time between failures and mean time to recovery provide an appropriate and effective indication of filter performance, avoiding spurious scoring and comparisons arising from current methods. The diagnosis of operational causes of elevated filtrate turbidity were framed as a machine learning classification problem which is a more efficient and scalable approach than traditional manual

interpretation of turbidity time series. The CART algorithm is demonstrated to be an effective diagnostic method generating highly accurate models describing conditions associated with elevated filtrate turbidity. Weekly models for individual filters and monthly models across the whole filter bank typically described conditions associated with elevated turbidity with accuracy over 90%.

By engineering and using operationally relevant predictor variables these diagnostic models were intuitive to interpret and translate into operational and preventative maintenance decisions. A weekly model for an individual filter was shown to clearly identify and communicate that elevated turbidity was largely associated with hydraulic loads greater than 1.2 times the within run average after 36.8 h of operation or hydraulic shocks greater than 1.1 times the within run average after 42.4 h of operation. Identifying these conditions clearly indicates that filter run times or hydraulic load fluctuations late in the run should be reduced. A monthly model describing performance across the filter bank identified that high turbidity occurred during the ripening of all filters and that turbidity breakthrough was an issue after 15 h except where filters were hydraulically underloaded compared to their neighbours. Furthermore, Filter D exhibited elevated turbidity earlier in the run during clarified turbidity spikes. Such conditions indicate that flow balancing, and the optimisation of pre-treatment and backwashing should be investigated to deliver performance improvements. The methods described can be readily applied to inform operational and preventative maintenance decisions.

Acknowledgements

The authors would like to thank the Engineering and Physical Sciences Research Council (Grant No: EP/G037094/1) and Scottish Water for their support of this work.

References

- [1] S. Rizak, S. Hrudey, Strategic Water Quality Monitoring for Drinking Water Safety, Salisbury, Australia, 2007.
- [2] B. Barbeau, V. Gauthier, A.-M. Bernier, R. Millette, G. Tremblay, Impact of raw water turbidity fluctuations on drinking water quality in a distribution system, *J. Environ. Eng. Sci.* 2 (2003) 281–291, <http://dx.doi.org/10.1139/s03-026>.
- [3] P.M. Huck, B.M. Coffey, M.B. Emelko, D.D. Maurizio, R.M. Slawson, W.B. Anderson, J. Van den Oever, Effects of filter operation on cryptosporidium removal, *J. Am. Water Works Assoc.* 94 (2002) 97–111.
- [4] P.J. Lusardi, P.J. Consonery, Factors affecting filtered water turbidity, *J. Am. Water Works Assoc.* 91 (1999) 28–40. <http://www.awwa.org/publications/journal-awwa/abstract.aspx?articleid=14140> (accessed January 15, 2014).
- [5] P. Foladori, L. Bruni, S. Tamburini, V. Menapace, G. Ziglio, Surrogate parameters for the rapid microbial monitoring in a civil protection module used for drinking water production, *Chem. Eng. J.* 265 (2015) 67–74, <http://dx.doi.org/10.1016/j.cej.2014.12.010>.
- [6] C.W. Anderson, Turbidity, in: *Natl. F. Man. Collect. Water-Quality Data (TWRI B. 9)*, ninth ed., USGS, 2005, pp. 1–55.
- [7] M.W. LeChevallier, T.M. Evans, R.J. Seidler, Effect of turbidity on chlorination efficiency and bacterial persistence in drinking water, *Appl. Environ. Microbiol.* 42 (1981) 159–167. <http://jaem.asm.org/content/42/1/159.short> (accessed June 4, 2014).
- [8] W.F. McCoy, B.H. Olson, Relationship among turbidity, particle counts and bacteriological quality within water distribution lines, *Water Res.* 20 (1986) 1023–1029.
- [9] The Scottish Ministers, The Water Supply (Water Quality) (Scotland) Regulations 2001, Scottish Parliament, 2001.
- [10] WHO, Guidelines for Drinking-Water Quality, fourth ed., World Health Organization, 2015.
- [11] EPA, Optimising Water Treatment Plant Performance Using the Composite Correction Program, EPA, 1998.
- [12] P.M. Huck, M.B. Emelko, B. Coffey, D. Maurizio, C.R. O'Melia, Filter Operation Effects on Pathogen Passage, AWWA, 2001.
- [13] J. Gregory, Cryptosporidium in water: treatment and monitoring methods, *Filtr. Sep.* 31 (1994) 268–289, [http://dx.doi.org/10.1016/0015-1882\(94\)80395-1](http://dx.doi.org/10.1016/0015-1882(94)80395-1).
- [14] B. Martin, Treatment Plant & Distribution System Optimization Programs Annual Data Summary Report, Denver, 2014.
- [15] G. Logsdon, A. Hess, M.J. Chipps, A. Rachwal, Filter Maintenance and Operations Guidance Manual, American Water Works Association, 2002.
- [16] L. DeMers, J. LeBlanc, Louisiana systems take on the optimization challenge, *J. Am. Water Works Assoc.* 95 (2003) 48–52.
- [17] A. Egerton, T. Hall, M. Watts, Statistical Process Control and Other Techniques for Managing Cryptosporidium Risk in Water Treatment, 1999.
- [18] T. Li, P.M. Huck, Improving the evaluation of filtration robustness, *J. Environ. Eng. Sci.* 7 (2008) 29–37.
- [19] A.J. Hartshorn, G. Prpich, A. Upton, J. Macadam, B. Jefferson, P. Jarvis, Assessing filter robustness at drinking water treatment plants, *Water Environ. J.* 44 (2014) 1–26.
- [20] V. Venkatasubramanian, R. Rengaswamy, K. Yin, A review of process fault detection and diagnosis Part I: Quantitative model-based methods, *Comput. Chem. Ellipsis* 27 (2003) 293–311.
- [21] V. Gitis, I. Rubinstein, M. Livshits, G. Ziskind, Deep-bed filtration model with multistage deposition kinetics, *Chem. Eng. J.* 163 (2010) 78–85.
- [22] H. Yuan, A.A. Shapiro, A mathematical model for non-monotonic deposition profiles in deep bed filtration systems, *Chem. Eng. J.* 166 (2011) 105–115.
- [23] V. Venkatasubramanian, R. Rengaswamy, S.N. Ka, A review of process fault detection and diagnosis Part II: Qualitative models and search strategies, *Comput. Chem. Eng.* 27 (2003) 313–326.
- [24] V. Venkatasubramanian, R. Rengaswamy, S.N. Ka, Y. Kewen, A review of process fault detection and diagnosis Part III: Process history based methods, *Comput. Chem. Eng.* 27 (2003) 327–346.
- [25] T. Hastie, R. Tibshirani, J. Friedman, *The Elements of Statistical Learning: Data Mining, Inference, and Prediction*, second ed., Springer-Verlag, 2009.
- [26] M. Kuhn, K. Johnson, Classification trees and rule-based models, in: *Appl. Predict. Model*, Springer, New York, NY, 2013, pp. 369–413, http://dx.doi.org/10.1007/978-1-4614-6849-3_14.
- [27] W. Thoe, M. Gold, A. Griesbach, M. Grimmer, M.L. Taggart, a.B. Boehm, Predicting water quality at Santa Monica Beach: evaluation of five different models for public notification of unsafe swimming conditions, *Water Res.* 67C (2014) 105–117.
- [28] L. Frederick, J. VanDerslice, M. Taddie, K. Malecki, J. Gregg, N. Faust, W.P. Johnson, Contrasting regional and national mechanisms for predicting elevated arsenic in private wells across the United States using classification and regression trees, *Water Res.* 91 (2016) 295–304.
- [29] L. Breiman, J. Friedman, C. Stone, R. Olshen, *Classification and Regression Trees*, CRC Press, 1984.
- [30] R Core Team, R: A Language and Environment for Statistical Computing <https://www.r-project.org/>2015.
- [31] RStudio Team, RStudio: Integrated Development Environment for R <http://www.rstudio.com/>2012.
- [32] PostgreSQL Global Development Group, PostgreSQL, 2015, 9.4.
- [33] G. Grolemund, H. Wickham, Dates and Times Made Easy with {lubridate}, *J. Stat. Softw.* 40 (2011) 1–25.
- [34] H. Wickham, Ggplot2: Elegant Graphics for Data Analysis, Springer, New York, 2009. <http://had.co.nz/ggplot2/book>.
- [35] H. Wickham, R. Francois, dplyr: A Grammar of Data Manipulation, 2015.
- [36] J. Conway, D. Eddelbuettel, T. Nishiyama, S.K. Prayaga, N. Tiffin, RPostgreSQL: R Interface to the PostgreSQL Database System, 2013.
- [37] M.K.C. Jed Wing, S. Weston, A. Williams, C. Keefer, A. Engelhardt, T. Cooper, Z. Mayer, B. Kenkel, the R Core Team, M. Benesty, R. Lescarbeau, A. Ziem, L. Scrucca, Y. Tang, C. Candan, caret: Classification and Regression Training, 2015. <https://cran.r-project.org/package=caret>.
- [38] T.M. Therneau, E.J. Atkinson, An Introduction to Recursive Partitioning Using the RPART routines, 2015, pp. 1–62.
- [39] A.M. Hurst, M.J. Edwards, M. Chipps, B. Jefferson, S.A. Parsons, The impact of rainstorm events on coagulation and clarifier performance in potable water treatment, *Sci. Total Environ.* 321 (2004) 219–230.
- [40] K. Zhang, G. Achari, R. Sadiq, C.H. Langford, M.H.I. Dore, An integrated performance assessment framework for water treatment plants, *Water Res.* 46 (2012) 1673–1683.
- [41] G. James, D. Witten, T. Hastie, R. Tibshirani, *An Introduction to Statistical Learning*, Springer, New York, 2013.
- [42] O.A.Z. Sotomayor, D. Odloak, Observer-based fault diagnosis in chemical plants, *Chem. Eng. J.* 112 (2005) 93–108, <http://dx.doi.org/10.1016/j.cej.2005.07.001>.
- [43] S. Han, C.S.B. Fitzpatrick, A. Wetherill, The impact of flow surges on rapid gravity filtration, *Water Res.* 43 (2009) 1171–1178.
- [44] J.L. Cleasby, M.M. Williamson, E.R. Baumann, Effect of filtration rate changes on quality, *J. Am. Water Works Assoc.* 55 (1963) 869–880.
- [45] S. Suthaker, D.W. Smith, S.J. Stanley, Optimisation of filter ripening sequence, *Aqua*, vol. 47, 1998.
- [46] J.E. Tobiasson, C.R.O. Melia, Physicochemical aspects of particle removal in depth filtration, *J. Am. Water Works Assoc.* 80 (1988) 54–64.
- [47] H.S. Kim, T.S. Moon, Y.J. Kim, M.S. Kim, W.H. Piao, S.J. Kim, C.W. Kim, Evaluation of rule-based control strategies according to process state diagnosis in A₂/O process, *Chem. Eng. J.* 222 (2013) 391–400, <http://dx.doi.org/10.1016/j.cej.2013.02.078>.
- [48] K. Tidriri, N. Chatti, S. Verron, T. Tiplica, Bridging data-driven and model-based approaches for process fault diagnosis and health monitoring: a review of researches and future challenges, *Annu. Rev. Control.* 42 (2016) 63–81, <http://dx.doi.org/10.1016/j.arcontrol.2016.09.008>.
- [49] C. Foscoliano, S. Del Vigo, M. Mulas, S. Tronci, Predictive control of an activated sludge process for long term operation, *Chem. Eng. J.* 304 (2016) 1031–1044, <http://dx.doi.org/10.1016/j.cej.2016.07.018>.